Localization of peripheral autonomic neurons innervating the boar urinary bladder trigone and neurochemical features of the sympathetic component

L. Ragionieri,[1] M. Botti,[1] F. Gazza,[1] C. Sorteni,[2] R. Chiocchetti,[2] P. Clavenzani,[2] L. Bo Minelli,[1] R. Panu[1]

[1]Department of Veterinary Science, University of Parma;
[2]Department of Veterinary Medical Science, University of Bologna, Italy

Abstract

The urinary bladder trigone (UBT) is a limited area through which the majority of vessels and nerve fibers penetrate into the urinary bladder and where nerve fibers and intramural neurons are more concentrated. We localized the extramural post-ganglionic autonomic neurons supplying the porcine UBT by means of retrograde tracing (Fast Blue, FB). Moreover, we investigated the phenotype of sympathetic trunk ganglia (STG) and caudal mesenteric ganglia (CMG) neurons positive to FB (FB+) by coupling retrograde tracing and double-labeling immunofluorescence methods. A mean number of 1845.1±259.3 FB+ neurons were localized bilaterally in the L1-S3 STG, which appeared as small pericarya (465.6±82.7 μm^2) mainly localized along an edge of the ganglion. A large number (4287.5±1450.6) of small (476.1±103.9 μm^2) FB+ neurons were localized mainly along a border of both CMG. The largest number (4793.3±1990.8) of FB+ neurons was observed in the pelvic plexus (PP), where labeled neurons were often clustered within different microganglia and had smaller soma cross-sectional area (374.9±85.4 μm^2). STG and CMG FB+ neurons were immunoreactive (IR) for tyrosine hydroxylase (TH) (66±10.1% and 52.7±8.2%, respectively), dopamine beta-hydroxylase (DβH) (62±6.2% and 52±6.2%, respectively), neuropeptide Y (NPY) (59±8.2% and 65.8±7.3%, respectively), calcitonin-gene-related peptide (CGRP) (24.1±3.3% and 22.1±3.3%, respectively), substance P (SP) (21.6±2.4% and 37.7±7.5%, respectively), vasoactive intestinal polypeptide (VIP) (18.9±2.3% and 35.4±4.4%, respectively), neuronal nitric oxide synthase (nNOS) (15.3±2% and 32.9±7.7%, respectively), vesicular acetylcholine transporter (VAChT) (15±2% and 34.7±4.5%, respectively), leu-enkephalin (LENK) (14.3±7.1% and 25.9±8.9%, respectively), and somatostatin (SOM) (12.4±3% and 31.8±7.3%, respectively). UBT-projecting neurons were also surrounded by VAChT-, CGRP-, LENK-, and nNOS-IR fibers. The possible role of these neurons and fibers in the neural pathways of the UBT is discussed.

Introduction

The urinary bladder (UB) stores and periodically releases urine under the control of neural circuits located in the brain, spinal cord and peripheral ganglia. The site in which the majority of nerve fibers and vessels penetrate the UB[1,2] and where nerve fibers and intramural neurons are more concentrated,[3,4] is the urinary bladder trigone (UBT). It is a dorsal triangular area of the UB, delimited by the ureteral and urethral orifices and lined by an epithelium classically deemed of mesodermal origin,[5] but whose endodermal origin has been recently suggested.[6] Recent studies suggest that the trigone is formed predominantly from the bladder muscle, and the contribution from ureteral longitudinal fibers is more limited.[7]

The UBT may be considered as forming a functional entity that controls urine outflow during filling and voiding, also providing an effective anti-reflux mechanism to prevent the backflow of urine into the ureters.[8] Therefore, it plays a vital role in maintaining continence and aiding micturition. Moreover, the UBT represents an elective site for cancer proliferation, in both veterinary[9,10] and human[11] medicine. Hence, we believe that the knowledge of UBT nervous pathways is essential for a better insight into the control of bladder storage and voiding in health and disease. It can provide a more complete understanding of the mode of action of existing therapies, and a basis for the development of future therapeutic approaches to maintain or regain a properly functioning of the UB.

Until now only sensory neurons[12] innervating the bladder and the neurons located in the intramural ganglia of porcine UBT[4] or in the pelvic part of the urethra and in the UB neck[13] have been thoroughly identified and studied. We have thus undertaken a study, combining retrograde neuronal tracing and standard immunohistochemical techniques, to provide a detailed description of the distribution, morphology and chemical coding of the peripheral sensory and autonomic neurons supplying porcine UBT. Data regarding sensory neurons have already been published.[14] In the present paper we describe the distribution and morphology of the extramural autonomic neurons and the chemical coding of a subset of sympathetic neurons supplying porcine UBT.

Correspondence: Luisa Ragionieri, Department of Veterinary Medical Science, University of Parma, via del Taglio 10, Parma, Italy.
Tel. +39.0521.032644 - Fax: +39.0521.032642.
E-mail: luisa.ragionieri@unipr.it

Key words: immunohistochemistry, retrograde tracing, peripheral autonomic neurons, urinary bladder trigone, pig.

Acknowledgments: the authors would like to thank Prof. Stefano Zanichelli and Dr. Fabio Leonardi for the surgical and anesthesiological support.

Contributions: all authors contributed equally to the work.

Received for publication: 27 November 2012.
Accepted for publication: 4 March 2013.

European Journal of Histochemistry 2013; 57:e16
doi:10.4081/ejh.2013.e16

We have chosen the domestic pig as experimental animal because it has been regarded as a more suitable model for studying human lower urinary tract innervation than rodents or carnivores.[15-18]

Materials and Methods

All the procedures described below were carried out in accordance with the European Communities Council Directive of 24 November 1986 (86/609/EEC) and the Italian legislation regarding experimental animals, after approval by the Scientific Ethics Committee for Experiments on Animals of the University of Parma (Prot. Rif. 68/09). All possible efforts were made to minimize the number of animals used and their suffering.

Four intact male crossbreed (Large white x Landrace x Duroc) pigs (aged 3 months, mean body weight: 34±3 Kg, range 30-38 Kg) were maintained on a diet and water *ad libitum* for 1 week before the experiment. For 24 h prior to surgery, the animals were not given any food and preventive antibiotic therapy with Ceftiofur (Naxcel 5 mg/Kg i.m., Pfizer, Sandwich Kent, UK) was administered. The animals were sedated by intramuscular injection of azaperone (4-10 mg/10 Kg, Stresnil, Janssen Cilag SpA, Cologno Monzese, Italy) and ketamine (150 mg/10 Kg, Ketavet 100, Intervet Italia Srl, Aprilia, Italy). After recum-

bency and venous catheterization (*vena auricularis lateralis*), anesthesia was induced by the administration of propofol (2-6 mg/Kg i.v., Rapinovet, Schering Plough, Segrate, Italy) and maintained with 1.5% to 2% isofluorane in 100% oxygen delivered by an open circuit, via a cuffed Magill orotracheal tube. The post-operative anti-inflammatory effect was achieved by an intramuscular injection of tolfedine (2 mg/kg, Vetoquinol S.A., Magny-Vernois, France) and analgesia was ensured with buprenorphine (10 mg/kg i.m., Temgesicl, Schering Plough, Segrate, Italy), administered daily (for 5 days) post operatively. The pigs were positioned in dorsal recumbency and the surgical field was prepared with Betadine and isopropyl alcohol scrub. A midline 10-12 cm post-umbilical laparotomy was performed. After visualization of the dorsal surface of the UB, 50 µL of fluorescent tracer Fast Blue (FB; Sigma-Aldrich Chemie, Steinheim, Germany; 2% aqueous solution) were carefully injected, by means of a manually operating glass Hamilton microsyringe, into five sites of the UBT. The microsyringe needle was inserted under the serosa in the middle of the trigonal area and close to the junction of each ureter with the UB, at a similar distance between the places of the injections. Injection sites were recognizable by observing the tracer's deposit beneath the serosa. To avoid leakage, the needle was left in place for about one minute. The wall of the injected organ was then rinsed with physiological saline and gently wiped with gauze. The viscera were replaced correctly and the abdomen closed using a routine three-layer suture procedure. The recovery and post operative periods were uneventful. Two weeks after surgery, the pigs were deeply sedated and anaesthetized as described above and subjected to euthanasia by i.v. administration of embutramide, mebenzonium iodide and tetracaine hydrochloride (Tanax, Intervet Italia, Segrate, Italy; 0.3 mL/kg).

The animals used in this study had 14 thoracic (Th), 7 lumbar (L), 4 sacral (S), and 20 caudal (Ca) vertebrae.

Specificity of the injection sites

Macroscopic and microscopic examinations of the sites of FB injections were performed before collecting the samples. They were easily identified by the yellow-labeled deposition generally left by the tracer at the injections sites. To verify that the tracer had not migrated into the urethra, we analyzed, in cryosections and by means of the H&E staining technique, the junction between the UBT and cranial portion of the urethra. In all four subjects the tracer was confined within the smooth musculature of the UBT. To verify whether the tracer was spreading into the urethral striated muscle, we also evaluated the absence of FB-labeled (FB+) neurons in the last lumbar (L7) and in the S1-S3 spinal cord (SC) segments which could contain pudendal efferent neurons innervating the striated perineal muscles correlated to micturition, defecation, and copulation (as described in Russo *et al*.[14]).

In these segments, we only observed a few preganglionic neurons located in the intermedio-lateral nucleus along the S3-S4 metameres of SC, which we interpreted as preganglionic autonomic parasympathetic cells connected to the numerous intramural ganglia documented[4] in the wall of the UBT.

Tissue preparation

From each subject we collected, on both sides, the sympathetic trunk ganglia (STG), the cranial and caudal mesenteric ganglia (CrMG and CMG), the pelvic plexus (PP), the SC and the dorsal root ganglia (DRG). The segmental ganglia and the SC were collected from Th11 to Ca2. The PP was identified and collected according to the indications provided by Tsaknakis,[19] Panu *et al*.,[20] and Sienkiewicz.[21] Data regarding the DRG have already been published elsewhere.[14]

All the samples collected were fixed for 6-8 h in 4% paraformaldehyde in phosphate buffer (0.1 M, pH 7.2) at 4°C, rinsed overnight in phosphate-buffered saline (PBS: 0.15 M NaCl in 0.01 M sodium phosphate buffer, pH 7.2) and stored at 4°C in PBS containing 30% sucrose and sodium azide (0.1%). The following day, the tissues were transferred to a mixture of PBS-30% sucrose-azide and Killik cryostat embedding medium (Bio-Optica, Milan, Italy) at a ratio of 1:1 for an additional 24 h before being embedded in 100% embedding medium. The sections were prepared by freezing the tissues in isopentane cooled in liquid nitrogen. Each ganglion was placed flat in the cryostat mould and serially cut into 16 µm thick sections along its longest axis, in order to obtain a large number of cells per section. The PP was cut into small samples serially sectioned. The SC was instead serially sectioned transversely and used, as indicated above, to control the specificity of the injection site. The serial sections from all samples were mounted on gelatine-coated slides (not coverslipped) and examined under a fluorescent microscope (Zeiss Axioskop 2 plus) equipped with epi-illumination and a filter system (excitation wavelength 390-420 nm; emission wavelength 450 nm) to reveal FB fluorescent labeling of neuronal cytoplasm. The slides were then stored at –80°C, and, from time to time, selected for IHC.

Quantitative analysis

The number of FB+ neurons was calculated by counting, in the sections, only the cells in which the nucleus was recognizable. The number of FB+ neurons was calculated by applying Abercrombie's formula;[22] the correction factor utilizes the T/T+h ratio, where T= section thickness (16 m) and h= mean diameter of the objects (nuclei of FB+ cells) along the perpendicular axis to the plane of the section. The mean diameter of the nuclei of 100 FB+ neurons for lumbar and sacral STG, CMG and PP neuronal classes, was calculated. The mean diameter of the lumbar and sacral STG neuronal nuclei did not show significant differences (see below) and was 11.6±1.1 µm; the correction factor was 0.57. The mean diameter of the CMG neuronal nuclei was 13.6±1.4 µm, and the correction factor 0.53. The mean diameter of the PP neuronal nuclei was 10±1.4 µm and the correction factor 0.61.

Both the total number of cells counted in STG, CMG and PP and the relative frequency of perykaria from either side of each segmental level were presented as mean ± standard error of the mean (SEM) for the four animals. In order to measure soma size, random sections, separated at least 80 µm from each other, were projected at a magnification of 40X and photographed with a Zeiss Axiocam MRc5 digital camera. For each neuronal class, the soma cross-sectional areas of at least two hundred labeled cells, in each animal, were established by means of the digital image processing software AxioVision release 4.5 (Carl Zeiss, MicroImaging GmbH, Germany), which calculates the area enclosed by a manually traced outline of the cell bodies. We presupposed that two hundreds cells could be sufficient to obtain a statistically significant mean size that would be reliable and comparable among the different districts. No attempt to correct possible over- or under-estimation was made during the image processing, so care was taken to take measurements in identical conditions.

Morphometric data relative to each neuronal class were compared within each animal and among animals by a one-way analysis of variance (ANOVA) test followed by the Tukey *post-hoc* test. The statistical significant level was set as $P<0.05$. All analyses were made with SPSS for Windows (v.18; SPSS Inc., Chicago, IL, USA).

Immunohistochemistry

We carried out the immunohistochemical investigation on the sympathetic trunk ganglia (STG) and caudal mesenteric ganglia (CMG), which are considered typical sympathetic ganglia,[23-26] and not on the ganglia of the pelvic plexus (PP) which are considered mixed autonomic ganglia containing both sympathetic and parasympathetic neurons.[26,27]

The STG and the CMG were stained by a double labeling immunofluorescence method to test the occurrence of calcitonin gene-relat-

ed peptide (CGRP), dopamine beta-hydroxylase (DβH), leu-enkephalin (LENK), neuronal nitric oxyde synthase (n-NOS), neuropeptide Y (NPY), somatostatin (SOM), substance P (SP), tyrosine hydroxylase (TH), vesicular choline acetyl transferase (VAChT), and vasoactive intestinal polypeptide (VIP), and the co-localization of TH with each of the other substances tested. The same combinations of primary antisera were applied to sections at least 160 µm away from each other to eliminate the likelihood of testing the same neuron twice for the same antisera. After air-drying at room temperature (RT) for 30 min, the sections were incubated with a solution containing 0.25% Triton X-100, 1% bovine serum albumin and 10% normal goat serum in phosphate-buffered saline (PBS: 0.15M NaCl in 0.01 M sodium phosphate buffer, pH 7.2) for 1 h (RT), to reduce non-specific background staining. They were then incubated with a combination of the primary antisera (overnight, RT) listed in Table 1, further incubated with a mixture of fluorescein isothiocyanate (FITC)-conjugated goat anti-rabbit IgG and biotinylated-goat anti-mouse IgG (1 h; RT) and, finally, incubated with Texas Red-conjugated streptavidin (1 h; RT) (primary antisera and secondary reagents are listed in Table 1) and mounted in buffered glycerol. The sections were rinsed with PBS for 5 min after each step of the immunolabeling process. The labeled sections were analyzed and photographed with a Zeiss Axioskop 2 plus fluorescence microscope equipped with epi-illumination and appropriate filters for FB, FITC (excitation wavelength 450-490 nm; emission wavelength 515-565 nm) and Texas Red (excitation wavelength 530-585 nm; emission wavelength 615 nm). Relationships between FB distribution and immunohistochemical staining were examined directly by interchanging filters. The observations were made by a single operator.

In each ganglion, the relative percentages of UBT-projecting neurons containing different combinations of the markers were calculated on the total number of FB+ cells tested for each couple of primary antisera. Data are expressed as means ± SEM between the four animals. Differences in the proportions of the various combinations of the markers in the different ganglia were evaluated by the chi-square test. A P value of <0.05 was considered significant. All analyses were made with SPSS for Windows (v.18; SPSS Inc., Chicago, IL, USA).

Antibody characterization

Specificity of the primary antibodies

The specificity of the anti-CGRP (Sigma-Aldrich) and anti-nNOS (Chemicon-Millipore) antibodies has been recently tested by Western blot (WB) analysis[14] on porcine tissues.

The specificity of the anti-TH (Sigma-Aldrich), anti-DβH (Chemicon), anti-SOM (Genetex), anti-NPY (Sigma-Aldrich) and anti-VAChT (Sigma Aldrich) antibodies was tested in the present research by WB analysis. Furthermore the anti-VIP antibodies, as well as anti-CGRP, -NPY, -TH, and -VIP antibodies were tested by adsorption test. It is also noteworthy that the Sigma-Aldrich datasheets state the specificity of anti-CGRP, -SP, -NPY, and -VIP antibodies for porcine tissues. WB failed to test the specificity of the polyclonal anti-LENK (Chemicon) antibody. In fact, the Chemicon datasheet specified that the product cannot be employed for this application. However no immunoreactivity was detected in a control experiment carried out, incubating sections in the absence of primary antiserum replaced by PBS. LENK is an opiod peptide derived from the same mammalian precursor,[28] thus it is reasonable to believe that the anti-LENK utilized in the present research recognizes the pig polypeptide.

Western blotting

Tissue samples (porcine DRG, STG and SC) were collected, frozen in liquid nitrogen, and stored at –80°C. Subsequently, for protein analysis, tissues were thawed and homogenized directly into a SDS lysis solution (Tris-HCl 62.5 mM pH 6.8; SDS 2%, 5% glycerol) with 0.1 mM phenylmethylsulfonylfluoride (PMSF). The protein content of cellular lysates was determined by a Protein Assay Kit (TP0300, Sigma-Aldrich Co, St. Louis, MO, USA). Aliquots containing 10 g proteins were separated on NuPage 4-12% bis-Tris Gel (Gibco-Invitrogen, Paisley, UK) for 50 minutes at 200V. Proteins were then electrophoretically transferred onto a nitrocellulose membrane. Blots were washed in PBS and protein transfer was checked by staining the nitrocellulose membranes with 0.2% Ponceau Red. After blocking treatment, the membranes were incubated at +4°C overnight with the respective antibodies in Tris Buffered Saline-T20 (TBS-T20 20mM Tris-HCl, pH 7.4, 500 mM NaCl, 0.1% T-20): anti-TH mouse monoclonal antibody (1:1500 Sigma Aldrich), anti-SOM rabbit polyclonal antibody (1:2000 GeneTex), anti-NPY rabbit polyclonal antibody (1:3000 Sigma Aldrich and Chemicon), anti-DβH rabbit polyclonal antibody (1:1000 Chemicon), anti-VAChT rabbit polyclonal (1:500 Sigma Aldrich), anti-LENK rabbit polyclonal (1:1000 Chemicon). After several washings with PBS-

Table 1. Antisera and dilutions used in the experiments.

Primary antibody	Raised in	Code no.	Dilution	Supplier
Anti-tyrosine hydroxylase (TH)	Mouse (monoclonal)	T 2928	1:4000	Sigma, St. Louis, MO, USA
Anti-dopamine hydroxylase (DβH)	Rabbit (polyclonal)	AB 1585	1:2000	Chemicon International, Inc., Temecula, CA, USA
Anti-vesicular choline acetyl transferase (VAChT)	Rabbit (polyclonal)	V 5387	1:500	Sigma, St. Louis, MO, USA
Anti-neuronal nitric oxyde synthase (n-NOS)	Rabbit (polyclonal)	AB 5380	1:1500	Chemicon International, Inc., Temecula, CA, USA
Anti-calcitonin gene related peptide (CGRP)	Rabbit (polyclonal)	C 8198	1:4000	Sigma, St. Louis, MO, USA
Anti-leu-enkephalin (LENK)	Rabbit (polyclonal)	AB1974	1:1000	Chemicon International, Inc. Temecula, CA, USA
Anti-neuropeptide Y (NPY)	Rabbit (polyclonal)	N 9528	1:4000	Sigma, St. Louis, MO, USA
Anti-somatostatin 28 (SOM)	Rabbit (polyclonal)	GTX11103	1:2500	GeneTex, Inc., Irvine, CA, USA
Anti-substance P (SP)	Rabbit (polyclonal)	S 1542	1:4000	Sigma, St. Louis, MO, USA
Anti-vasoactive intestinal polypeptide (VIP)	Rabbit (polyclonal)	V 3508	1:4000	Sigma, St. Louis, MO, USA
Secondary antibody	**Raised in**	**Code no.**	**Dilution**	**Supplier**
Anti-rabbit IgG/FITC	Goat	F 0382	1:40	Sigma, St. Louis, MO, USA
Anti-mouse IgG/Biotin	Sheep	RPN 1001	1:100	Amersham Pharmacia Biotech, Little Chalfont, UK
Streptavidin/Texas Red		RPN 1233	1:100	Amersham Pharmacia Biotech, Little Chalfont, UK

T20 the membranes were incubated with the secondary biotin-conjugated antibody and then with a 1:1000 dilution of an anti-biotin horseradish peroxidase (HRP)-linked antibody. The Western blots (WB) were developed using chemiluminescent substrate (Super Signal West Pico Chemiluminescent Substrate, Pierce Biotechnology, Inc, Rockford, IL, USA) according to the manufacturer's instructions. The intensity of the luminescent signal of the resulting bands was captured by Fluor-STM Multimager using Quantity One Software (Bio-Rad Laboratories Inc., Hercules, CA, USA). WB analysis confirmed the specificity of the primary antibodies utilized in the present study.

The band revealed in the spinal cord by the anti-TH antibody showed a molecular weight of approximately 58 kDa (Figure 1) while in the DRG the band showed a lower molecular weight of approximately 55kDa (Figure 1); since the complete protein sequence in pigs is not available (http://www.uniprot.org), we considered the theoretical molecular weight of TH in *Homo sapiens* (58kDa). In *Homo sapiens* four isoforms of the protein are known, 55.6, 56, 58.1, and 58.5 kDa; we cannot exclude that two specific isoforms of this protein might exist in the pig. WB analysis for DβH protein showed, in porcine spinal cord and DRG, a band of approximately 70 kDa; although the sequence of DβH seems to be preserved among different species, such as mammals and birds, the complete sequence of DβH in swine is not available. As observed also in other species,[29-31] we found a monomeric and a dimeric isoform of DβH (Figure 1). WB analysis for somatostatin protein, in porcine spinal cord (but not in the DRG), determined a band of approximately 13 kDa (Figure 1), consistent with the weight of pre-propeptide. WB analysis for NPY protein, in porcine spinal cord, showed a band of approximately 11 kDa (Figure 1), consistent with the complete sequence of pre-propeptide. In the DRG the band was weaker (*data not shown*), and showed a different molecular weight (approximately 4,5 kDa), in line with the result reported by Kos *et al*.[32] WB analysis for VAChT protein showed, in porcine STG, a band of approximately 70 kDa (Figure 1) consistent with the weight of the sequence of aminoacids of VAChT.

Results

The use of the retrograde neuronal tracer enabled us to locate UBT-projecting neurons in each category of the samples collected.

Sympathetic trunk ganglia

The labeled cells of the STG were found consistently in the bilateral L1-S3 ganglia. The mean number of FB+ neurons was 1845.1±259.3, mostly (86.5±5.2%) located in L7-S2 ganglia. The frequency distribution of FB+ neurons in each segmental level of the STG is shown in Figure 2. Labeled neurons were isolated or clustered in small groups of 2-3 neurons scattered throughout the individual ganglia. In the ganglia containing the highest number of labeled cells, the latter were almost exclusively localized along an edge of the ganglion with an obvious topographical organization (Figure 3, A1). Labeled cells were typical multipolar neurons (Figure 3, A2), showing an elliptical shape with the longer axis generally oriented parallel to the longitudinal axis of the ganglion. Labeled neurons showed the nucleus eccentrically placed. As we failed to find significant differences between the sizes of lumbar and sacral STG neurons within each animal, or among animals, we pooled all the measures of STG neurons of the four subjects. The mean value of the soma cross-sectional areas of UBT-projecting neurons in the STG was of 465.6±82.7 μm^2. We compared this mean value with those of the CMG and PP FB+ neurons (see below) and found significant differences (one-way ANOVA test, $P<0.001$). The results are shown in Figure 4.

Cranial mesenteric ganglia

Of all the samples examined there was only one positive response (8 FB+ neurons) in a left CrMG. The small number of cells observed did not allow us to make significant statistical evaluations or morphological descriptions.

Caudal mesenteric ganglia

The mean number of FB+ neurons found in the bilateral CMG was 4287.5±1450.6, with the majority of these cells (65.7±13.5%) located in the left ganglion.

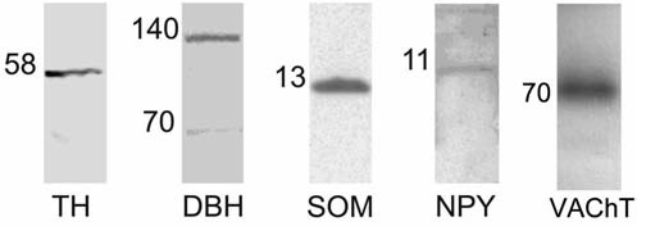

Figure 1. Western blot immunolabeling of tyrosine hydroxylase, dopamine beta-hydroxylase, somatostatin, neuropeptide Y and vesicular acetylcholine transporter in porcine dorsal root ganglia, sympathetic trunk ganglia and spinal cord. The number on the left of each line indicates the molecular weight. The images of the different immunoblots were slightly adjusted in brightness and contrast to provide a uniform background. TH: tyrosine hydroxylase; DβH: dopamine beta-hydroxylase; NPY: neuropeptide; VAChT: vesicular acetylcholine transporter.

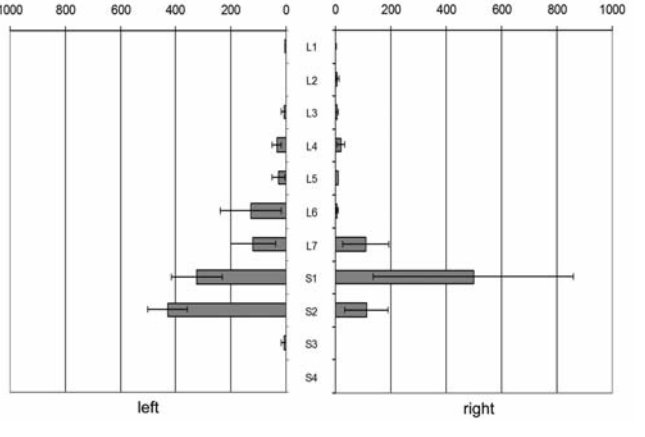

Figure 2. Histogram showing the frequency distribution of urinary bladder trigone-projecting neurons (mean total number 1845.1±259.3, n=4) in each segmental level of the sympathetic trunk ganglia.

Labeled cells were almost exclusively found along an edge of the CMG with an apparent topographical organization (Figure 3, B1). These cells were typical multipolar neurons (Figure 3, B2), with their longer axis generally oriented parallel to the longitudinal axis of the ganglion. Neurons were generally oval and readily identifiable by their large rounded nucleus. As the mean value of their cross-sectional areas did not show significant differences between the four subjects, we pooled together all the measures of CMG UBT-projecting neurons from all the animals, for a total of 476.1±103.9 μm² (Figure 4). The resulting mean value was not significantly different from the one of the STG UBT-projecting neurons (Tukey *post-hoc* test, P>0.05).

Pelvic plexus

Traced somata were found constantly in the PP; in fact, a mean number of 4793.3±1990.8 FB+ neurons were found in the bilateral part of the pelvic plexus, located in the angle between the urethral end of the deferens ducts and the cranial part of the vesicular gland. The majority (61.1±12.9%) of these cells was isolated or clustered within the right micro-ganglia. Labeled pelvic cells were typical multipolar neurons (Figure 3, C1-C2) and the mean value of their soma cross-sectional areas did not show significant differences between the four subjects: therefore we pooled all the measures of PP UBT-projecting neurons of the four subjects, for a total of 374.9±85.4 μm² (Figure 4). This value was significantly smaller than what resulted for CMG and STG (Tukey *post-hoc* test P<0.05).

Immunohistochemistry of sympathetic ganglia

We carried out the immunohistochemical investigation on the sympathetic trunk ganglia (STG) and caudal mesenteric ganglia (CMG).

Sympathetic trunk ganglia

Each combination of primary antisera was tested on a mean number of 235.7±22 FB+ neurons from each animal. The percentages of FB+ cells immunoreactive (-IR) for only one of the markers employed or co-expressing also TH-immunoreactivity are reported in Figure 5. The average percentage of FB+ neurons showing TH-immunoreactivity was 66±10.1% and the vast majority (92±7.1%) of these cells co-expressed DβH-immunoreactivity, indicating a catecholaminergic nature (Figure 6, A1-A3). As many as 59±8.2% of FB+ neurons were NPY-IR, while 52.3±7.2% of them co-expressed

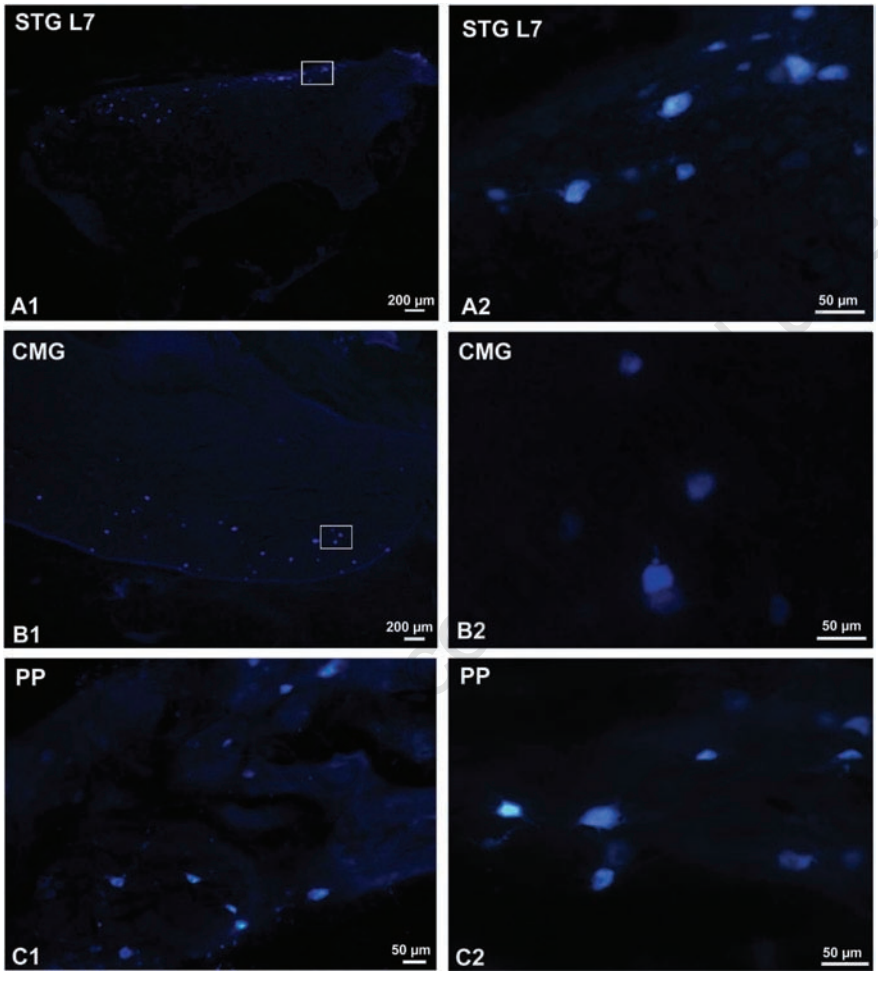

Figure 3. A) Photomicrographs of the longitudinal section of the L7 right sympathetic trunk ganglion (STG L7), one of the ganglia containing the highest density of Fast Blue (FB)-labeled cells innervating the pig urinary bladder trigone. A1) Distribution of the FB-labeled sympathetic postganglionic neurons at the ganglion periphery as visible at low magnification (1x); the white rectangle indicates the area where the image shown in A2 has been taken from. A2) Morphology of the sympathetic postganglionic neurons labeled, as visible at higher magnification (20x). B) Photomicrographs of the longitudinal section of the right caudal mesenteric ganglion (CMG). B1) Distribution of the FB-labeled sympathetic postganglionic neurons at the ganglion periphery as visible at low magnification (1x); the white rectangle indicates the area where the image shown in B2 has been taken from. B2) Morphology of the same labeled neurons as visible at higher magnification (20x). C) Photomicrographs of a section of one micro-ganglion of the pelvic plexus (PP) showing the distribution of the postganglionic FB-labeled neurons (C1). C2) Morphology of the PP labeled neurons as visible at higher magnification (20x).

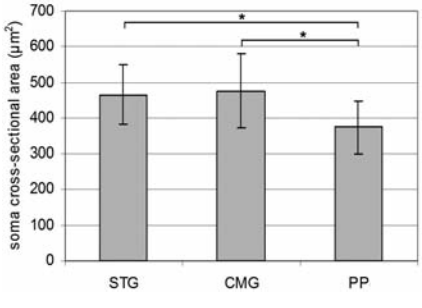

Figure 4. Mean sizes (±SEM, n=4 pigs) of urinary bladder trigone-projecting postganglionic neurons in the sympathetic trunk ganglia (STG), caudal mesenteric ganglia (CMG) and pelvic ganglia (PP). The soma cross sectional area was measured on at least two hundred FB-labeled cells from each neuronal class in each animal. One-way ANOVA analysis revealed significant differences (P<0.001) between the mean sizes of neurons in the three kind of ganglia. Asterisks in the figure indicate a positive significance level (*P<0.05) obtained in the comparison of PP *vs* CMG and STG with Tukey *post-hoc* test.

TH- and NPY-immunoreactivity was 52.3±7.2% (Figure 6, B1-B3). UBT-projecting neurons also showed positivity for all the other markers used, in the following percentages: CGRP- (24.1±3.3%), SP- (21.6±2.4%), VIP- (18.9±2.3%), nNOS- (15.3±2%), VAChT- (15±2%), LENK- (14.3±7.1%), and SOM-IR (12.4±3%). In addition, FB+ TH-IR neurons co-expressed CGRP- (20±2.3%) (Figure 6, C1-C3), SP- (18.6±5.3%), VIP- (14.6±2.4%), VAChT- (15±2%), nNOS- (12.1±3.4%), SOM- (11.5±4.2%) (Figure 6, D1-D3), and LENK-immunoreactivity (10.5±3.2%).

VAChT- (Figure 7A), CGRP-, LENK-IR (Figure 7B) and, to a lesser extent, nNOS-IR fibers formed varicosities around the FB+ neurons.

Caudal mesenteric ganglia

Each combination of primary antisera was tested on a mean number of 487.1±48.2 FB+ neurons of the CMG from each animal. The percentages of FB+ cells immunoreactive for only one antiserum or co-expressing immunoreactivity for an antiserum and TH, are reported in Figure 5.

On average, about half of FB+ neurons (52.7±8.2%) showed immunoreactivity for TH and the vast majority (86.5±6.2%) of them co-expressed DβH-immunoreactivity, indicating the catecholaminergic nature of these neurons. The majority (65.8±7.3%) of FB+ neurons were NPY-IR, whereas 57.9±5.9% co-expressed TH-and NPY-immunoreactivity. UBT-projecting neurons also showed positivity for all the other markers used, in the following percentages: CGRP- (22.1±3.3%), SP- (37.7±7.5%), VIP- (35.4±4.4%), nNOS- (32.9±7.7%), VAChT- (34.7±4.5%), LENK- (25.9±8.9%) and SOM-IR (31.8±7.3%). In addition, FB+ TH-IR neurons co-expressed CGRP- (17.9±4.8%), SP- (33.7±7.3%) (Figure 8, A1-A3), VIP- (32.1±1.5%) (Figure 8, B1-B3), VAChT- (23.4±3.3%) (Figure 8, C1-C3), nNOS- (22.6±6.1%) (Figure 8, D1-D3), SOM- (27.1±4.2%) and LENK-immunoreactivity (23.3±2.5%) (Figure 8, E1-E3). VAChT-, CGRP- (Figure 7C), LENK-IR and, to a lesser extent, nNOS-IR (Figure 7D) fibers formed varicosities around FB+ neurons.

Discussion

Localization

The postganglionic neurons projecting to the UBT were found bilaterally in the L1-S3 STG (87±5% of them in L7-S2 ganglia), in the CMG and the PP. On the contrary, very few cells were observed in the CrMG. Our findings are in accordance with what is commonly known about the innervation of the UB. In fact, it is well recognized that the UB is supplied by three sets of peripheral nerves: i) hypogastric nerves - mainly containing sympathetic postganglionic fibers, a few preganglionic fibers supplying the so called *short adrenergic neurons* in the ganglia located very close to pelvic organs[4,33,34] and sensory, mainly nociceptive, fibers[12,14]; ii) pelvic nerves - consisting mainly of preganglionic fibers, supplying the parasympathetic neurons of the PP and the intramural ganglia, as well as the postganglionic[16,35-38] and sensory, mainly mechanoceptive,[14] fibers; iii) sacral spinal sensory nerves (pudendal nerves[39,40]).

We can hypothesize that all the autonomic fibers that reach the UBT pass through the PP. In particular, the few fibers originating in the lumbar STG (L1-L6) travel along the hypogastric nerves, together with those originating in the CMG, to reach the PP and supply the UBT, while most of the fibers originating in the lumbo-sacral STG (L7-S2) likely travel along the pelvic nerves to reach the PP, join its postganglionic fibers and supply the UBT. Another interesting finding was the somatotopic localization of the labeled neurons in the STG mostly involved in the innervation of the UBT (STG L7-S1-S2) and in the CMG, whereas, in the other STG, small amounts of FB+ neurons were scattered throughout the individual ganglia and no obvious topographical organization was detected. Several studies have already proven, in the pig as well as in other species, a clear somatotopic organization of prevertebral ganglion neurons supplying different organs.[23,26,41,42] On the contrary, in pig STG, a somatotopic organization of visceral-projecting neurons has already been observed only for colon-projecting neurons[43]. In fact, it is commonly accepted that neurons with specific functions or projection fields are not highly localized within the STG, although there is a general rostrocaudal organization of neurons with respect to the position of their targets along the rostrocaudal axis of the body. This is correlated with the exit sites of the neurons from the ganglion[44,45] and is due to the fact that STG contain relatively large populations of neurons generally involved in the same function (*e.g.*, vasomotor perikarya).

We have also provided information regarding soma size of the traced perykaria. This information reflects a comparative rather than a representative value of the real cell size among the different categories of neurons. Autonomic neurons were generally small (area 1000 μm^2 and diameter 40 μm); in particular, in the PP the FB+ neurons were smaller than those in the STG and CMG. This may be due to their being located closer to the UBT, or to the low level of circulating androgens typical of three months old pigs[46] (like the ones used in the present study). In fact the androgen effects

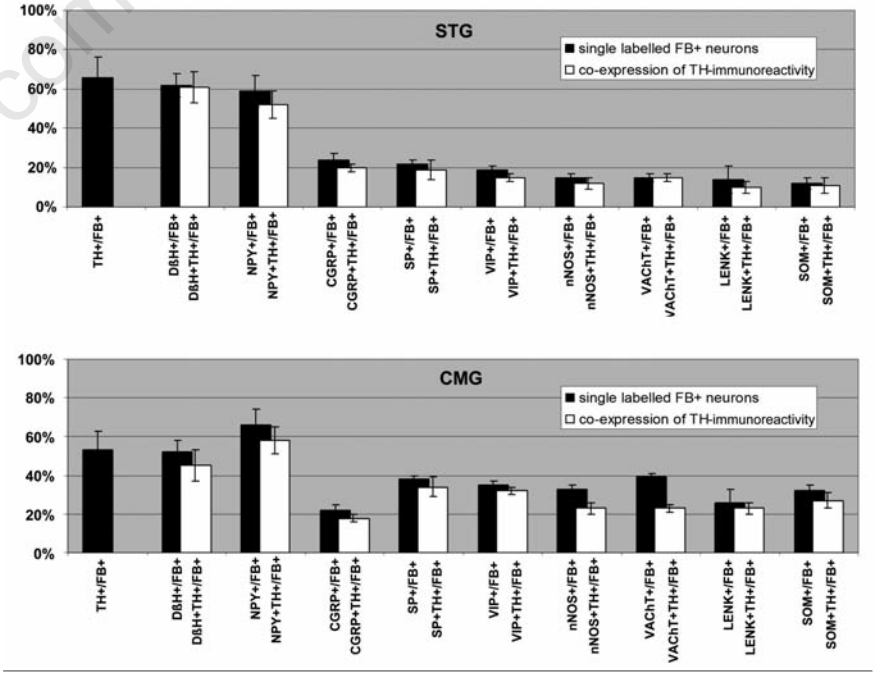

Figure 5. Histograms showing the mean ± SEM percentages (n=4 pigs) of sympathetic trunk ganglia (STG) and caudal mesenteric ganglia (CMG) neurons projecting to the pig UBT (FB+ neurons) immunoreactive (+) to each antiserum and the proportion of these FB+ neurons that co-expressed also TH-immunoreactivity (TH+).

on neuron morphology are not restricted to neurons with a direct role in reproductive reflexes, but also impact upon the neurons involved in bladder and bowel function.[47]

Immunohistochemistry

Tyrosine hydroxylase and/or dopamine beta-hydroxylase immunoreactivity

In the STG, the immunohistochemical staining revealed that about 60% of UBT-projecting neurons showed an adrenergic (TH/DβH-IR) phenotype and preferentially co-expressed NPY. In the CMG, the percentage of adrenergic neurons was smaller (about 45%). Furthermore, TH/NPY-IR cells represented about 60% of UBT-projecting neurons. Although large neurons (with diameter ranging between 40 and 65 µm) were present in the STG observed, the adrenergic and NPY-IR UBT-projecting neurons were small (area <1000 µm^2 and diameter 40 µm) and preferentially located at the ganglion periphery.

Perhaps the most unexpected finding of our study was the not so high percentage of immunoreactivity to TH and DβH. In fact, previous immunohistochemical investigations revealed that, in the pig, as in other mammals, the vast majority of STG[48] and CMG[49,50] neurons are noradrenergic in nature. We believe that the differences observed in our results may be related to the age of the animals used in our experiments. In fact, it is known that the immunohistochemical properties of sympathetic neurons can change with age[51] and that the autonomic neurons innervating the genital organs,[52,53] and some bladder- or bowel-projecting neurons are influenced by steroid hormones.[53,54] The low level of serum testosterone, documented by Colenbrander *et al.*[46] in three-month old boars, could explain the relatively small percentages of adrenergic neurons found in our study, compared with those that project to the male or female genital organs of sexually mature (of more than 100 Kg and 8 months of age) sows[55] or boars.[52]

The particular target tissue should also be taken into consideration in explaining our findings. In fact, the percentages of adrenergic neurons observed are similar to the ones reported by Pidusdko[4] in the intramural autonomic neurons found in the trigone of 10 kg-weighting gilts. Therefore, the adrenergic neurons projecting to pig UBT might be not very numerous in the STG and in the CMG because another subpopulation of adrenergic neurons is present in the UBT intramural ganglia. The chemical content and particular distribution of labeled neurons and their rather small size suggest that they have a vasoconstrictor function, according to earlier research conducted on other species.[26,56-59] However, vasoconstriction may not be the only possible function for the labeled catecholaminergic neurons observed. In fact, Larsen *et al.*[60] and Lakomy *et al.*[61] found in porcine UBT a very high number of adrenergic nerve fibers apparently related to the smooth myocytes of the muscular tunic in the UB as well as to myocytes of the tunica media in the blood vessels supplying this organ. Thus, the adrenergic UBT-projecting neurons should have also a visceromotor function. The role of the visceromotor adrenergic neurons on the UBT smooth muscle appears complex. According to Yamanishi *et al.*[18], the functional role of the bladder base, including the bladder trigone, is to open and close the bladder neck during filling and emptying, respectively. The superficial trigonal layer, composed of smooth muscle of mesodermal origin, is thought to be sensitive to noradrenaline, with responses being predominantly mediated by α-adrenoceptors.[18,62,63] During bladder filling, the adrenergic stimulation causes the contraction of the superficial layer to keep the bladder neck closed. The deep trigonal layer, which is instead of endodermal origin, like the detrusor muscle,[18] responds to the same noradrenergic stimuli by β-adrenoceptors, relaxing and not opposing the closure of the bladder neck, but favoring flattening and elongation of the bladder base.[18] During emptying, the detrusor and the deep layer of the trigone respond to acetylcholine via muscarinic receptors by contracting and facilitating the opening of the bladder neck.[64,65]

Neuropeptide Y immunoreactivity

The possible role of NPY within noradrenergic neurons has already been discussed above. In general, NPY could have a role in the inhibi-

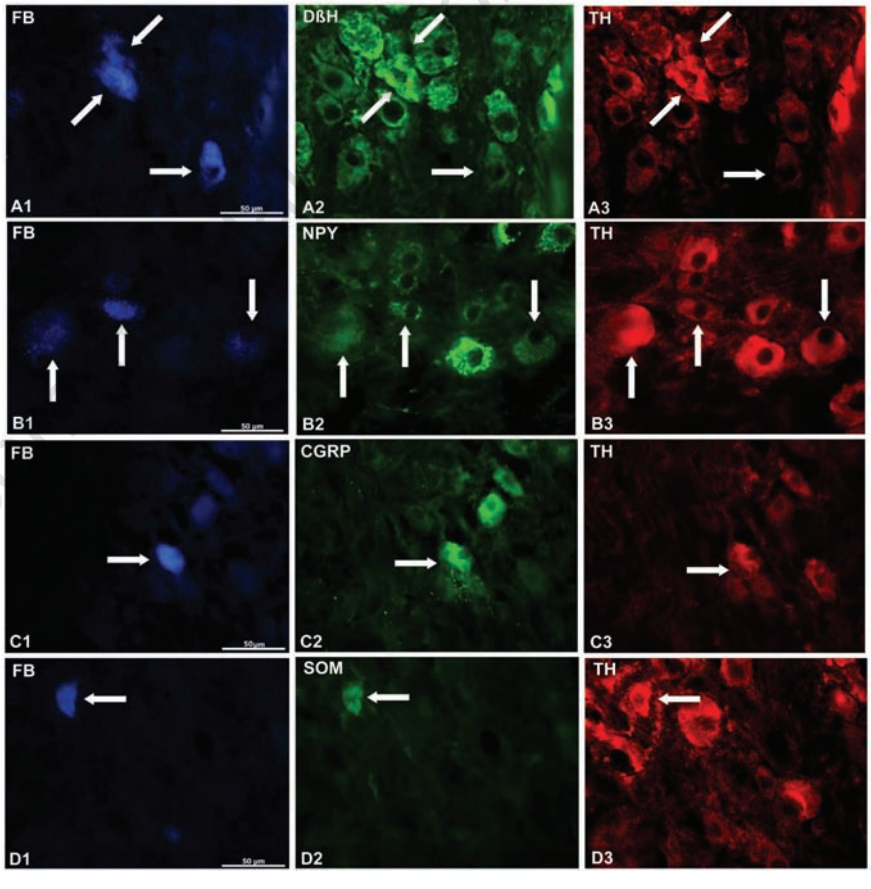

Figure 6. Fluorescence micrographs of longitudinal sections of the porcine sacral (S1) sympathetic trunk ganglion containing FB-positive perikarya double labeled for TH and one of the different markers employed. In the group of figures labeled with the letter A, the arrows indicate three FB-positive perikarya (A1) containing simultaneously DβH (A2) and TH (A3). In the group of figures labeled with the letter B, the arrows indicate three FB-positive cell bodies (B1) double immunolabeled for NPY (B2) and TH (B3). In the group of figures labeled with the letter C, the arrow points to a FB-positive cell body (C1) which simultaneously contained CGRP (C2) and TH (C3). In C2, near this cell, are also visible varicose CGRP-immunolabeled nerve fibers. Finally, in the group of figures labeled with the letter D, the arrow points to a FB-positive cell body (D1) containing simultaneously SOM (D2) and TH (D3).

tion of non-adrenergic-non-cholinergic (NANC), adrenergic and cholinergic excitatory neurotransmission, as already hypothesized by Persson *et al.*[66] who observed few to moderate numbers of NPY-IR terminals related to muscle bundles or the surrounding small arteries in the lamina propria of the trigone of adult female pigs.

Vesicular acetylcholine transporter immunoreactivity

VAChT-immunoreactivity, alone or co-localized with TH-immunoreactivity, indicates that, besides pelvic ganglia[49] and parasympathetic intramural neurons[4,67] sympathetic para- and prevertebral neurons can also be the source of the high number of AChE-positive nerves observed in the pig trigone, in both the submucosal layer and in the muscular layer.[66,67] The number of cholinergic neurons we observed in the ganglia is small, but this might be also due to the limited availability and sensitivity of a suitable marker for cholinergic neurons in the peripheral nervous system.[23,68] Another reason could be that, in many species, including the pig, choline acetyltranferase- (ChAT-) and VAChT-immunoreactivity are present in a number of endothelial cells[69] and in non-neuronal cells within the urothelium,[70,71] suggesting that there may be other sources of acetylcholine with a role in some regulatory mechanisms. The co-localization of cholinergic and catecholaminergic markers has already been observed in STG neurons projecting to the pig bulbospongiosus muscle,[72] to the retractor penis muscle in the male pig[73], and to the sow retractor clitoridis muscle.[74] Moreover, ChAT and DßH were found co-localized in the cranial cervical ganglion of fetal pig.[75] It is known that, during fetal development, some neurons transiently express the noradrenergic phenotype but subsequently lose their noradrenergic characteristics, becoming cholinergic cells.[76-78] If so, we hypothesize that, in the sympathetic neurons observed herein, the development of the cholinergic marker might not be paralleled by a complete disappearance of the various catecholamine markers.

In the trigone the function of cholinergic innervation might be the presynaptic modulation of the adrenergic excitatory neurotransmission.[70]

Calcitonin-gene-related peptide immunoreactivity

CGRP is commonly considered a marker of afferent pathways;[79-81] therefore, its presence within STG neurons could appear an unusual finding and its co-localization with TH even more so. However, the detection of CGRP-IR in TH-negative neurons has already been described in pig STG,[72,82,83] and the co-localization of CGRP with TH has also been observed in a small number of STG neurons projecting to the pig bulbospongiosus muscle[72] and to the sow rectractor clitoridis muscle.[74] Persson *et al.*[66] observed a small number of varicose CGRP-IR fibers in the muscular layer of the UBT, with only very few being perivascular. A moderate number of CGRP-IR fibers has also been observed to supply neurons in the porcine UBT intramural ganglia.[4] These fibers were interpreted as collaterals of sensory neurons in the urinary tract, which may modulate smooth muscle activity by an antidromic efferent function; however, we have proven that there is also a small contribution of autonomic ganglia to the peptidergic innervation of the UBT. In accordance with Häppölä *et al.*,[82] we hypothesize that they play a functional role in the modulation of neurotransmission in target organs of porcine sympathetic ganglia.

Substance P immunoreactivity

Although many researchers have always considered SP to be absent in neurons of pig STG[43,82,83] and CMG,[50] we have already proven the presence of SP alone in a very small number of paravertebral neurons projecting to the pig retractor penis muscle,[73] and of SP co-localized with TH in the STG neurons projecting to the pig bulbospongiosus muscle[72] and the sow retractor clitoridis muscle.[74] The same co-localisation has already been observed in a moderate number of neurons of UBT intramural ganglia.[4] Considering the potent vasodilatory action of SP, the functional significance of its presence in neurons devoid of TH might be their participation in blood-flow regulation.[84] The putative physiological significance of the

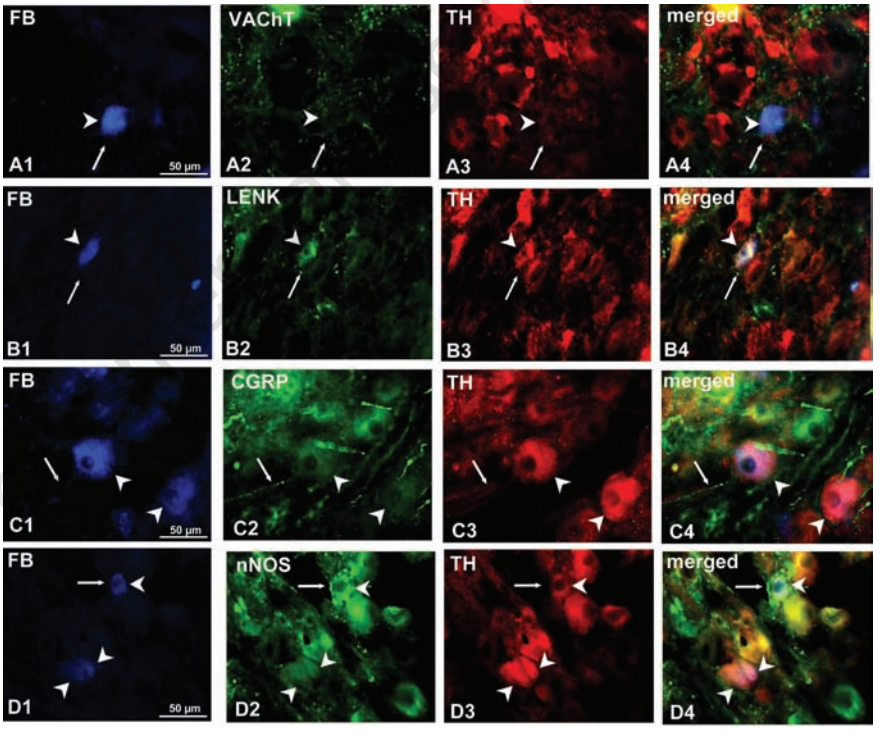

Figure 7. Microphotographs of sections from the porcine STG S1 (A1-B4) and CMG (C1-D4). A) the arrowhead shows an UBT-projecting neuron (FB-positive perikarion) (A1) immuno-negative for TH (A3, Texas Red visualisation) and VAChT (A2, FITC visualisation), but surrounded by a meshwork of nerve terminals (indicated by arrows) immunoreactive for VAChT (A2, FITC visualisation); these images were digitally superimposed in A4. B) the arrowhead shows a FB-positive neuron (B1) immunoreactive both for LENK (B2, FITC visualisation) and for TH (B3, Texas Red visualisation); single nerve fibres immunoreactive for LENK (FITC visualisation) are visible between the ganglion cells and indicated by arrow. These images were digitally superimposed in B4. C) arrowheads indicate two FB-positive neurons (C1) weakly immunoreactive for CGRP (C2, FITC visualisation) and TH (C3, Texas Red visualisation); single nerve fibres immunoreactive for CGRP (FITC visualisation) are visible between and on the ganglion cells and indicated by the arrow; these images were digitally superimposed in C4. D) arrowheads show three FB-positive neurons simultaneously immunostained for nNOS (D2, FITC visualisation) and TH (D3, Texas Red visualisation); nNOS-immunoreactive fibres (FITC visualisation) surrounding the ganglion cells are indicated by arrows; the images were digitally superimposed in D4 (double-labelled nerve cells are yellow).

co-existence of TH and SP might be their role in several visceral reflexes and neuroendocrine responses, as already hypothesized for other species.[79,85]

Vasoactive intestinal polypeptide immunoreactivity

Immunoreactivity for VIP has already been found, with distinct cranio-caudal differences, in some neurons of the pig cervical,[82] thoracolumbar[48,83] and sacral STG.[75] Quantitative differences in the positivity for this peptide have been found also within the pig UBT by different researchers. In fact, Pidsudko[4] failed to find any immunoreactivity for VIP in either intramural neurons or fibers in the UBT of juvenile female pigs, whereas Crowe and Burnstock[16] have described, in female adult pigs, the population of VIP-immunoreactive neurons as the second biggest of the UBT intramural ganglia. Persson *et al*.[66] also described VIP-immunoreactive nerve terminals accompanying muscle bundles as the most frequent in the muscle layer of the female adult pig trigone. Those authors attribute the differences in their results to the use of different antisera, animals of different age, or the procedure used. Therefore, our findings could also be explained by the fact that we used juvenile animals. VIP-ergic neurons could play a role in blood flow regulation, because, like NO, VIP acts as vasodilator on genital organ blood vessels[79,86,87] and displays a physiological antagonism with NPY in the control of blood flow.[87] In particular, in the pig it reduces the tension and amplitude of the spontaneous contractions of trigonal strips[88] and relaxes the bladder neck.[89] Also the distribution of VIP-containing nerves in the smooth muscle, around blood vessels and beneath the epithelium in the pig urinary tract[16] suggests that these VIP-IR neurons may participate in the regulation of smooth muscle activity, perhaps acting as local modulators of neuromuscular transmission, blood flow and epithelial activity.

The co-localization of TH and VIP has already been described in sacral STG neurons projecting to the pig bulbospongiosus muscle[72] and to the sow retractor clitoridis muscle[74]. Moreover VIP has already been found in association with DßH in some vasodilatory neurons of porcine thoracic sympathetic chain ganglia.[26,48] However, the coexistence of TH and VIP is unusual for a peptide commonly thought to be a marker of the cholinergic pathway or a classical neurotransmitter of the inhibitory non-adrenergic-non-cholinergic (NANC) subdivision of the autonomic nervous system;[89,90] in addition, according to Hill and Elde[48] these TH/VIP-IR neurons could have a vasodilatory action as well.

Neuronal nitric oxide synthase immunoreactivity

Several morphological and functional studies support a parasympathetic origin of NO in the lower urinary tract, as the localization of nitrergic fibers often coincided with that of nerves expressing acetylcholine esterase-, VIP- and NPY-immunoreactivity.[68] However, we recently demonstrated that NOS-IR innervation of the pig UBT may originate also from DRG neurons,[14] and the present study shows a minimal contribution of STG as well. NOS-IR innervation is particularly dense in the pig UBT and is present also in the smooth muscle layer[66] where it accompanies the muscle bundles and fibers surrounding small arteries and forming plexuses around them and surrounding the ganglionic nerve cells in the UBT intramural ganglia.[4] All these observations are in line with functional studies showing that NO may have a role in the inhibitory neurotransmission in the pig trigone and seems to be involved in the endothelium-dependent acetylcholine-induced relaxation of pig vesical arteries.[91,92] The physiological role of the neuronal NO-mediated vasodilatation in the bladder can only be speculated upon. The UB wall frequently undergoes changes in wall tension during filling, which may affect blood flow. If the blood flow decreases during bladder filling[93,94] an activation of the vasodilator mechanisms has to take place in order to supply oxygen to the detrusor muscle. The co-localization

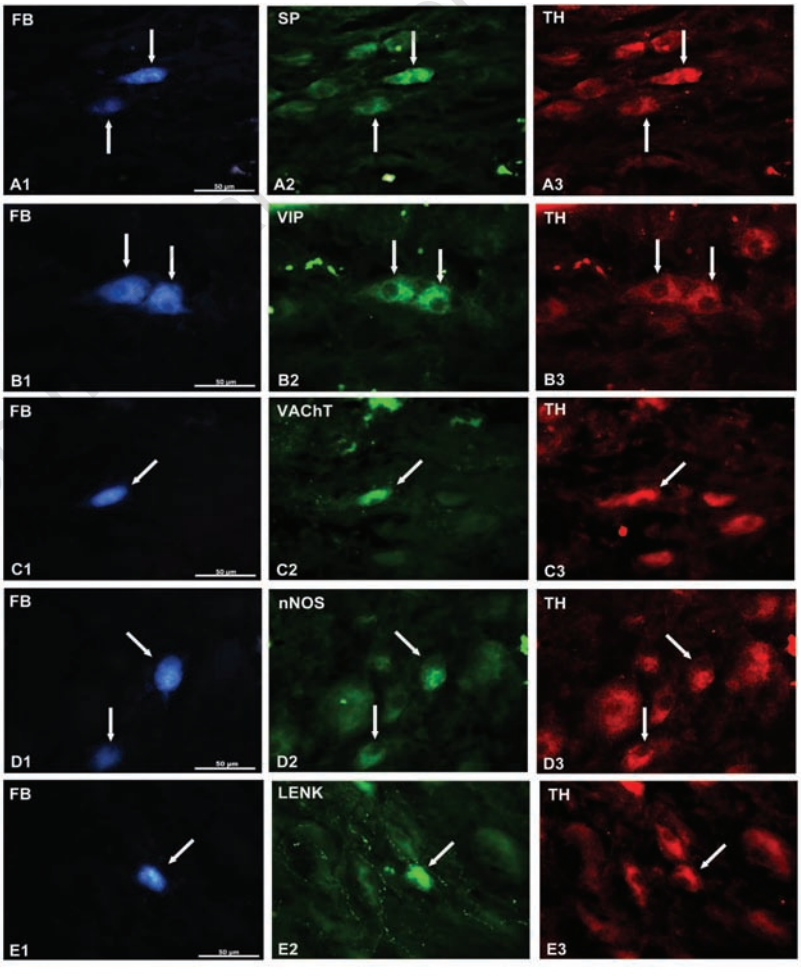

Figure 8. Microphotographs of sections from the porcine CMG containing FB-positive perikarya double labeled for TH and one of the different markers employed. A) Arrows indicate two FB-positive perikarya (A1) that simultaneously contained SP (A2) and TH (A3). B) Arrows indicate two FB-positive cell bodies (B1) double immunolabeled for VIP (B2) and TH (B3). C) Arrow points to a FB-positive cell body (C1) which simultaneously contained VAChT (C2) and TH (C3). D) Arrows indicate two FB-positive cell bodies (D1) which simultaneously contained nNOS (D2) and TH (D3). E) Arrows indicate two FB-positive cell bodies (E1) which simultaneously contained LENK (E2) and TH (E3).

of nNOS with TH had been observed earlier in some paravertebral neurons projecting to the bulbospongiosus muscle of the male pig[72] and to the retractor clitoridis muscle of the sow.[74] In its co-existence with TH, it might play a modulating role; in fact, it seems to induce an increase in TH activity in postganglionic neurons via both cyclic GMP-dependent and -independent mechanisms.[95]

Leu-enkephalin immunoreactivity

The LENK-IR and LENK/TH-IR neurons observed in the present study could represent one of the sources of the small number of varicose LENK-IR fibers found in the muscular layer of porcine trigone.[66] The co-existence of LENK or other enkephalins with TH in pig paravertebral neurons has been observed only in some neurons projecting to the pig bulbospongiosus muscle,[72] and to the sow retractor clitoridis muscle;[74] moreover, opioid peptides have been detected in noradrenergic nerve terminals supplying both the muscle layer and some arteries of the porcine oviduct.[96]

In the pig, the presence of opioid peptides has been noticed in the neurons of the cervical,[82] thoraco-lumbar[83] and sacral[72,73] STG, independently of the presence of TH. Moreover, LENK-immunoreactivity and, in general, opioid peptides have been seen in fibers innervating the pig female genital organs.[96,97] In agreement with Crowe and Burnstock,[16] LENK-IR neurons might have an inhibitory action on many intramural bladder neurons, or, more in general, a regulatory role in the neurotransmission in the UBT and its vessels. In fact, the co-existence of enkephalins with noradrenaline in sympathetic ganglia[98] and in fibers innervating the genital organs[99] suggests that these peptides may presynaptically modulate (inhibit) sympathetic inputs at the neuro-effector junction.[96,100] The same co-existence observed in several noradrenergic perivascular nerve fibers[101] suggests that enkephalins might also have a vasodilator effect due to their inhibitory action on autonomic neurotransmission.[23,80,98]

Somatostatin immunoreactivity

The SOM-IR and SOM/TH-IR neurons observed in the present study could represent one of the sources of the small number of varicose SOM-IR fibers found in the muscular layer of porcine trigone[66] or which supply the neurons in the intramural ganglia of the porcine UBT.[4] SOM-IR neurons have already been observed in porcine STG,[69,102] and both SOM/TH-IR and SOM-IR/TH-immunonegative neurons have been described in porcine CMG.[50] According to Lacroix *et al.*,[102] Majewski and Heym,[50] and Mayewski,[26] it is possible to hypothesize a vasoconstrictor role for these neurons.

Fibers supplying sympathetic urinary bladder trigone-projecting neurons

We observed FB+ neurons surrounded by VAChT-, CGRP-, LENK- and nNOS-IR fibers in both STG and CMG. The number and distribution of these fibers is quite similar to those already described by Skobowiat *et al.*[43] for the fibers surrounding colon-projecting neurons in pig STG, while the presence of VAChT-, CGRP- and LENK-IR fibers we observed in the CMG is in accordance with what already described by Kaleczyc *et al.*[49] in the CMG of male pigs.

The numerous VAChT-IR nerve fibers surrounding FB+ perikarya in STG and CMG, together, could originate presumably from preganglionic cholinergic neurons located in the intermediolateral nucleus of the spinal cord.[49,59] Moreover part of the LENK-IR nerve fibers encircling/neighbouring FB+ perikarya probably originate from STG neurons or constitute viscerofugal projections from the gut wall, because these specifically coded neurons were found in enteric ganglia, while they are scarce in the DRG of porcine male[103] and absent from the areas of the grey matter of the spinal cord containing autonomic nuclei.[49,104-106] The CGRP-IR nerve fibers observed may originate from DRG afferent neurons.[14,49,50,105,107] We think that the FB+/TH-IR perikarya supplied by petpidergic (especially LENK-IR) nerve fibers act as integrative neurons.[56,88] In fact, the neurons intensely supplied with LENK- or CGRP-IR nerve terminals could represent integrating (associative) nerve cells probably projecting to the viscera and receiving information from both the gastrointestinal tract via a centripetal projection pathway and from autonomic nuclei in the spinal cord.[49] Other smaller TH-IR neurons, supplied by VAChT-IR nerve fibers, probably contribute to the innervation of the uro-genital organs and blood vessels. The vast majority of CMG neurons projecting to porcine male uro-genital organs belong to this neuronal subpopulation.[49]

Finally, nNOS-IR fibers could originate from the preganglionic neurons located in the intermediolateral nucleus of the lumbar spinal cord or from DRG neurons.[14] Nitric oxide is present in more than one functional subpopulation of sympathetic preganglionic neurons and may have a role both as a directly acting transmitter, and as a modulator of efferent neurotransmission, besides being involved in afferent neurotransmission.[108-110] Therefore, even the nNOS-IR fibers that we observed around the UBT-projecting neurons could represent both centripetal projections from autonomic nuclei in the spinal cord, and collaterals of sensory neurons supplying sympathetic neurons with integrative functions.

Conclusions

The present study proves the involvement of different categories of autonomic ganglia in the innervation of porcine UBT. In particular, we demonstrated for the first time that, besides the well recognized contribution of the PP and CMG to the nervous control of the UBT, there is also a conspicuous participation of the sympathetic trunk, with a broad cranio-caudal extension of the STG involved, as already shown for the cat.[111] We have also documented that the chemical coding of sympathetic UBT-projecting neurons is quantitatively diversified, but qualitatively similar, in STG and CMG, where the neurons are not only adrenergic but also contain acetylcholine and different regulatory peptides. In particular, the substances with a regulating/modulating action appear to be more important than the classical neurotransmitters, *i.e.*, adrenaline or acethlcholine in neurons that innervate an area as that of the bladder base, characterized by highly complex structure and functions.

The knowledge of the different regulatory transmitters and peptides present in the sympathetic neurons innervating the UBT may result useful in the development of new therapies for the treatment of neurogenic disease of the urinary bladder, which should be modulated in relation to sex and age.

References

1. Fowler CJ, Griffiths D, de Groat WC. The neural control of micturition. Nat Rev Neurosci 2008;9:453-66.
2. Birder L, de Groat WC, Mills I, Morrison J, Thor K, Drake M. Neural control of the lower urinary tract: peripheral and spinal mechanisms. Neurourol Urodyn 2010;29: 128-39.
3. Andersson KE. Bladder activation: afferent mechanisms. Urology 2002;59:43-50.
4. Pidsudko Z. Distribution and chemical coding of neurons in intramural ganglia of the porcine urinary bladder trigone. Folia Histochem Cytobiol 2004;42:3-11.
5. McGaedy TA, QuinnPJ, FitzPatrick ES, Ryan MT. Veterinary embryology, urinary system. Oxford, UK, Blackwell Publishing Ltd., 2006; p 240.
6. Tanaka ST, Ishii K, Demarco RT, Pope JC IV, Brock JW III, Hayward SW. Endodermal origin of bladder trigone inferred from mesenchymal-epithelial interaction. J Urol 2010;183:386-91.
7. Viana R, Batourina E, Huang H, Dressler GR, Kobayashi A, Behringer RR, et al. The development of the bladder trigone, the

center of the anti-reflux mechanism. Development 2007;134:3763-9.
8. Tanagho EA. The ureterovesical junction. In G.D. Chisholm, D.I. Williams (eds.), Scientific foundations of urology, Heinemann, London, 1982; pp. 395-404.
9. Wilson HM, Chun R, Larson VS, Kurzman ID, Vail DM. Clinical signs, treatments, and outcome in cats with transitional cell carcinoma of the urinary bladder: 20 cases (1990-2004). J Am Vet Med Assoc 2007; 231:101-6.
10. Saulnier-Troff FG, Busoni V, Hamaide A. A technique for resection of invasive tumors involving the trigone area of the bladder in dogs: preliminary results in two dogs. Vet Surg 2008;37:427-37.
11. Shokeir AA. Squamous cell carcinoma of the bladder: pathology, diagnosis and treatment. BJU Int 2004;93:216-20.
12. Bossowska A, Crayton R, Radziszewski P, Kmiec Z, Majewski M. Distribution and neurochemical characterization of sensory dorsal root ganglia neurons supplying porcine urinary bladder. J Physiol Pharmacol 2009;60:77-81.
13. Sienkiewicz W, Kaleczyc J, Czaja K, Lakomy M. Adrenergic, nitrergic and peptidergic innervation of the urethral muscle in the boar. Folia Histochem Cytobiol 2004; 42:89-94.
14. Russo D, Clavenzani P, Sorteni C, Bo Minelli L, Botti M, Gazza F, et al. Neurochemical features of boar lumbosacral dorsal root ganglion neurons and characterization of sensory neurons innervating the urinary bladder trigone. J Comp Neurol 2013;521:342-66.
15. Larsen JJ. alpha and beta-adrenoceptors in the detrusor muscle and bladder base of the pig and beta-adrenoceptors in the detrusor muscle of man. Br J Pharmacol 1979;65:215-22.
16. Crowe R, Burnstock G. A histochemical and immunohistochemical study of the autonomic innervation of the lower urinary tract of the female pig. Is the pig a good model for the human bladder and urethra? J Urol 1989;141:414-22.
17. Yamanishi T, Chapple CR, Yasuda K, Yoshida K, Chess-Williams R. Identification of beta-adrenoceptor subtypes in lower urinary tract of the female pig. J Urol 2002;168:2706-10.
18. Yamanishi T, Chapple CR, Yasuda K, Yoshida K, Chess-Williams R. Role of beta-adrenoceptor subtypes in mediating relaxation of the pig bladder trigonal muscle in vitro. Neurourol Urodyn 2003;22:338-42.
19. Tsaknakis A. Morphological studies of the pelvic plexus of the pig. Zentralbl Veterinarmed A 1971;18:310-24.
20. Panu R, Bo Minelli L, Botti M, Gazza F, Acone F, Ragionieri L, et al. Localization of neurons projecting into the extrinsic penile smooth musculature of the pig: an experimental study on the retractor penis muscle. Anat Rec A Discov Mol Cell Evol Biol 2003;275:1102-8.
21. Sienkiewicz W. Sources of the porcine testis innervation. Andrologia 2010;42: 395-403.
22. Guillery RW. On counting and counting errors. J Comp Neurol 2002;447:1-7.
23. Kaleczyc J. Origin and neurochemical characteristics of nerve fibres supplying the mammalian vas deferens. Micr Res Tech 1998;42:409-22.
24. Kepper M, Keast J. Immunohistochemical properties and spinal connections of pelvic autonomic neurons that innervate the rat prostate gland. Cell Tissue Res 1995;281: 533-42.
25. Papka RE, Thompson BD, Schmidt HHHW. Identification of uterine-related sympathetic neurons in the rat inferior mesenteric ganglion: neurotransmitter content and afferent input. J Auton Nerv Syst 1996; 59:51-9.
26. Majewski M. Synaptogenesis and structure of the autonomic ganglia. Folia Morphol (Warsz) 1999;58:65-99.
27. Keast JR. Plasticity of pelvic autonomic ganglia and urogenital innervation. Int Rev Cytol 2006;248:141-208.
28. Noda M, Furutani Y, Takahashi H, Toyosato M, Hirose T, Inayama S, et al. Cloning and sequence analysis of cDNA for bovine adrenal preproenkephalin. Nature 1982; 295:202-6.
29. Fraeyman NH, Van de Velde EJ, De Smet FH. Molecular forms of dopamine beta-hydroxylase in rat superior cervical ganglion and adrenal gland. Experientia 1988; 44:746-9.
30. Russo D, Fantaguzzi CM, Di Guardo G, Clavenzani P, Costerbosa GL, Ligios C, et al. Characterization of sheep (Ovis aries) palatine tonsil innervation. Neuroscience 2009;161:813-26.
31. Russo D, Bombardi C, Grandis A, Furness JB, Spadari A, Bernardini C, et al. Sympathetic innervation of the ileocecal junction in horses. J Comp Neurol 2010; 518:4046-66.
32. Kos K, Harte AL, James S, Snead DR, O'Hare JP, McTernan PG, et al. Secretion of neuropeptide Y in human adipose tissue and its role in maintenance of adipose tissue mass. Am J Physiol Endocrinol Metab 2007;293:E1335-40.
33. Feher E, Vajda J. Sympathetic innervation of the urinary bladder. Acta Morphol Acad Sci Hung 1981;29:27-35.
34. Downie JW, Champion JA, Nance DM. A quantitative analysis of the afferent and extrinsic efferent innervation of specific regions of the bladder and urethra in the cat. Brain Res Bull 1984;12:735-40.
35. Crowe R, Haven AJ, Burnstock G. Intramural neurons of the guinea-pig urinary bladder: histochemical localization of putative neurotransmitters in cultures and newborn animals. J Auton Nerv Syst 1986; 15:319-39.
36. Gabella G. Intramural neurons in the urinary bladder of the guinea-pig. Cell Tissue Res 1990;261:231-7.
37. Lasanen LT, Tammela TL, Kallioinen M, Waris T. Effect of acute distension on cholinergic innervation of the rat urinary bladder. Urol Res 1992;20:59-62.
38. Uvelius B, Gabella G. The distribution of intramural nerves in urinary bladder after partial denervation in the female rat. Urol Res 1998;26:291-97.
39. De Groat WC, Booth AM Synaptic transmission in pelvic ganglia. In: CA Maggi (ed.) Nervous control of the urogenital system. Harwood Academic Publ., 1993; pp. 291-347.
40. De Groat WC, Booth AM, Yoshimura N. Neurophysiology of micturition and its modification in animal models of human disease. In: CA Maggi (ed.) Nervous control of the urogenital system. Harwood Academic Publ., 1993; pp. 227-290.
41. Kaleczyc J, Timmermans JP, Majewski M, Lakomy M, Scheuermann DW. Distribution and immunohistochemical characteristics of neurons in the porcine caudal mesenteric ganglion projecting to the vas deferens and seminal vesicle. Cell Tissue Res 1995;282:59-68.
42. Pidsudko Z, Kaleczyc J, Majewski M, Lakomy M, Scheuermann DW, Timmermans JP. Differences in the distribution and chemical coding between neurons in the inferior mesenteric ganglion supplying the colon and rectum in the pig. Cell Tissue Res 2001;303:147-58.
43. Skobowiat C, Calka J, Wasowicz K, Majewski M. Distribution pattern and chemical coding of neurons of the sympathetic chain ganglia supplying the descending colon in the pig. Acta Vet Hung 2010;58:189-98.
44. Flett DL, Bell C. Topography of functional subpopulations of neurons in the superior cervical ganglion of the rat. J Anat 1991; 177:55-66.
45. Luebke JI, Wright LL. Characterization of superior cervical ganglion neurons that project to the submandibular glands, the eyes, and the pineal gland in rats. Brain Res 1992;589:1-14.
46. Colenbrander B, de Jong FH, Wensing CJ. Changes in serum testosterone concentrations in the male pig during development.

J Reprod Fertil 1978;53:377-80.
47. Keast JR, Saunders RJ. Testosterone has potent, selective effects on the morphology of pelvic autonomic neurons which control the bladder, lower bowel and internal reproductive organs of the male rat. Neuroscience 1998;85:543-56.
48. Hill EL, Elde R. Vasoactive intestinal peptide distribution and colocalization with dopamine-beta-hydroxylase in sympathetic chain ganglia of pig. J Auton Nerv Syst 1989;27:229-39.
49. Kaleczyc J, Sienkiewicz W, Klimczuk M, Czaja K, Lakomy M. Differences in the chemical coding of nerve fibres supplying major populations of neurons between the caudal mesenteric ganglion and anterior pelvic ganglion in the male pig. Folia Histochem Cytobiol 2003;41:201-11.
50. Majewski M, Heym C. Immunohistochemical localization of calcitonin gene-related peptide and cotransmitters in a subpopulation of postganglionic neurons in the porcine inferior mesenteric ganglion. Acta Histochem 1992;92:138-46.
51. Maslyukov PM, Nozdrachev AD, Timmermans JP. Age-related characteristics of the neurotransmitter composition of neurons in the stellate ganglion. Neurosci Behav Physiol 2007;37:349-53.
52. Sienkiewicz W. Immunohistochemical properties of sympathetic chain ganglia (SChG) neurons projecting to the porcine testis in animals subjected to hemicastration, castration and testosterone supplementation. Pol J Vet Sci 2010;13:301-11.
53. Keast JR. The autonomic nerve supply of male sex organs--an important target of circulating androgens. Behav Brain Res 1999;105:81-92.
54. Keast JR. Effects of testosterone on pelvic autonomic pathways: progress and pitfalls. J Auton Nerv Syst 2000;79:67-73
55. Koszykowska M, Kozłowska A, Wojtkiewicz J, Skobowiat C, Majewski M, Jana B. Distribution and chemical coding of sympathetic neurons in the caudal mesenteric ganglion projecting to the ovary in sexually mature gilts. Acta Vet Hung 2010;58:389-403.
56. Heym C, Webber R, Horn M, Kummer W. Neuronal pathways in the guinea-pig lumbar sympathetic ganglia as revealed by immunohistochemistry. Histochemistry 1990;93:547-57.
57. Trudrung P, Furness JB, Pompolo S, Messenger JP. Locations and chemistries of sympathetic nerve cells that project to the gastrointestinal tract and spleen. Arch Histol Cytol 1994;57:139-50.
58. McLachlan EM. Autonomic ganglia. Harwood Academic Publishers, Luxemburg, 1995.
59. Gibbins IL, Morris JL. Pathway specific expression of neuropeptides and autonomic control of the vasculature. Regul Pept 2000;93:93-107.
60. Larsen JJ, Nordling J, Christensen B. Sympathetic innervation of the urinary bladder and urethral muscle in the pig. Acta Physiol Scand 1978;104:485-90.
61. Lakomy M, Kaleczyc J, Wasowicz K. Adrenergic innervation of the ureters, urinary bladder, and urethra in pigs. Gegenbaurs Morphol Jahrb 1989;135:347-55.
62. Caine M, Raz S, Zeigler M. Adrenergic and cholinergic receptors in the human prostate, prostatic capsule, and bladder neck. Br J Urol 1975;47:193-202.
63. Khanna OP, Barbieri E, AltamuraM, Mc Michael R. Vesicourethral smooth muscle: function and relation to structure. Urology 1981;118:211-8.
64. Dass N, McMurray G, Greenland JE, Brading AF. Morphological aspects of the female pig bladder neck and urethra: Quantitative analysis using computer assisted 3-dimensional reconstructions. J Urol 2001;165:1294-9.
65. Yamanishi T, Chapple CR, Yasuda K, Yoshida K, Chess-Williams R.The role of M2 muscarinic receptor subtypes in mediating contraction of the pig bladder base after cyclic adenosine monophosphate elevation and/or selective M3 inactivation. J Urol 2002;167:397-401.
66. Persson K, Alm P, Johansson K, Larsson B, Andersson KE. Co-existence of nitrergic, peptidergic and acetylcholine esterase-positive nerves in the pig lower urinary tract. J Auton Nerv Syst 1995;52:225-36.
67. Lakomy M, Wasowicz K, Kaleczyc J, Chmielewski S. AChE-positive innervation of the ureters, urinary bladder, and urethra in pigs. Z Mikrosk Anat Forsch 1990; 104:316-26.
68. Klimczuk M, Kaleczyc J, Franke-Radowiecka A, Czaja K, Podlasz P, Łakomy M. Immunohistochemical characterisation of cholinergic nerve fibres supplying accessory genital glands in the pig. Vet Med Czech 2005;50:119-30.
69. Haberberger RV, Bodenbenner M, Kummer W. Expression of the cholinergic gene locus in pulmonary arterial endothelial cells. Histochem Cell Biol 2000;113:379-87.
70. Sellers DJ, Chess-Williams R. Muscarinic agonists and antagonists: effects on the urinary bladder. Handb Exp Pharmacol 2012;375-400.
71. Ochodnicky P, Uvelius B, Andersson KE, Michel MC. Autonomic nervous control of the urinary bladder. Acta Physiol (Oxf) 2013;207:16-33.
72. Gazza F, Acone F, Botti M, Ragionieri L, Panu R, Bo Minelli L, et al. Double labelling immunohistochemistry on the peripheral autonomic neurons projecting to the bulbospongiosus muscle in male impuberal pigs. Vet Res Commun 2003; 27:603-5.
73. Botti M, Ragionieri L, Bo Minelli L, Gazza F, Acone F, Panu R, et al. Peripheral neurons innervating the extrinsic smooth penile musculature of the pig: experimental study by retrograde transport and immunohistochemistry. Ital J Anat Embryol 2006;111:65-82.
74. Ragionieri L, Botti M, Gazza F, Bo Minelli L, Acone F, Panu R, et al. Double labelling immunohistochemical characterization of autonomic sympathetic neurons innervating the sow retractor clitoridis muscle. Eur J Histochem 2008;52:29-38.
75. Wang JM, Partoens PM, Callebaut DP, Coen EP, Martin JJ, De Potter WP. Phenotype plasticity and immunocytochemical evidence for ChAT and D beta H co-localization in fetal pig superior cervical ganglion cells. Brain Res Dev Brain Res 1995;90:17-23.
76. Schafer MK, Weihe E, Erickson JD, Eiden LE. Human and monkey cholinergic neurons visualized in paraffin-embedded tissues by immunoreactivity for VAChT, the vesicular acetylcholine transporter. J Mol Neurosci 1995;6:225-35.
77. Keast JR. Unusual autonomic ganglia: connections, chemistry, and plasticity of pelvic ganglia. Int Rev Cytol. 1999;193:1-69.
78. Masliukov PM, Timmermans JP. Immunocytochemical properties of stellate ganglion neurons during early postnatal development. Histochem Cell Biol 2004; 122:201-9.
79. Majewski M, Kaleczyc J, Sienkiewicz W, Lakomy M. Existence and co-existence of vasoactive substances in nerve fibres supplying the abdomino-pelvic arterial tree of the female pig and cow. Acta Histochem 1995;97:235-56.
80. Kaleczyc J, Timmermans JP, Majewski M, Lakomy M, Scheuermann DW. Immunohistochemical characteristics of nerve fibres supplying the porcine vas deferens. A colocalisation study. Histochem Cell Biol 1997;107:229-41.
81. Czaja K. Distribution of primary afferent neurons innervating the porcine oviduct and their immunohistochemical characterization. Cells Tissues Organs 2000;166: 275-82.
82. Häppölä O, Lakomy M, Majewski M, Wasowicz K, Yanaihara N. Distribution of neuropeptides in the porcine stellate ganglion. Cell Tissue Res 1993;274:181-7.
83. Lakomy M, Häppölä O, Kaleczyc J, Majewski M. Immunohistochemical localization of neuropeptides in the porcine thoraco-lumbar paravertebral ganglia. Anat Histol Embryol 1994;23:12-20.

84. Lindh B, Lundberg JM, Hökfelt T. NPY-, galanin-, VIP/PHI-, CGRP- and substance P-immunoreactive neuronal subpopulations in cat autonomic and sensory ganglia and their projections. Cell Tissue Res 1989;256:259-73.
85. Traurig HH, Papka RE, Shew RL. Substance P and related peptides associated with the afferent and autonomic innervation of the uterus. Ann NY Acad Sci 1991;632:304-13.
86. Polak JM, Gu J, Mina S, Bloom SR. Vipergic nerves in the penis. Lancet 1981; 2:217-9.
87. Morris JL, Gibbins IL, Furness JB, Costa M, Murphy R. Co-localization of neuropeptide Y, vasoactive intestinal polypeptide and dynorphin in non-noradrenergic axons of the guinea pig uterine artery. Neurosci Lett 1985;62:31-7.
88. Klarskov P, Gerstenberg T, Hald T. Vasoactive intestinal polypeptide influence on lower urinary tract smooth muscle from human and pig. J Urol 1984;131:1000-4.
89. Yoshiyama M, de Groat WC. The role of vasoactive intestinal polypeptide and pituitary adenylate cyclase-activating polypeptide in the neural pathways controlling the lower urinary tract. J Mol Neurosci 2008; 36:227-40.
90. Itoh H, Sakai J, Imoto A, Creed KE. The control of smooth muscle tissues by nonadrenergic noncholinergic (NANC) nerve fibres in the autonomic nervous system. J Smooth Muscle Res 1995;31:67-78.
91. Persson K, Andersson KE. Nitric oxide and relaxation of pig lower urinary tract. Br J Pharmacol 1992;106:416-22.
92. Persson K, Alm P, Johansson K, Larsson B, Andersson KE. Nitric oxide synthase in pig lower urinary tract: immunohistochemistry, NADPH diaphorase histochemistry and functional effects. Br J Pharmacol 1993;110:521-30.
93. Dunn M. A study of the bladder blood flow during distension in rabbits. Br J Urol 1975; 47:67-72.
94. Kozlowski R, Siroky MB, Krane RJ, Azadzoi KM. Regulation of blood flow and microcirculation resistance in rabbit bladder. J Uro 2002;168:1608-14.
95. Klimaschewski L, Kummer W, Heym C. Localization, regulation and functions of neurotransmitters and neuromodulators in cervical sympathetic ganglia. Microsc Res Tech 1996;35:44-68.
96. Czaja K, Kaleczyc J, Sienkiewicz W, Majewski M, Lakomy M. Peptidergic innervation of the porcine oviduct studied by double-labelling immunohistochemistry. Folia Histochem Cytobiol 1996;34:141-50.
97. Gazza F, Botti M, Bo Minelli L, Ragionieri L, Acone F, Panu R, et al. Double labelling immunohistochemistry on the nerve fibres of retractor clitoridis muscle of the sow. Vet Res Commun 2005;29:191-4.
98. Konishi S, Tsunoo A, Otsuka M. Enkephalin as a transmitter for presynaptic inhibition in sympathetic ganglia. Nature 1981;294: 80-2.
99. De Potter WP, Coen EP, De Potter RW. Evidence for the coexistence and corelease of [Met]enkephalin and noradrenaline from sympathetic nerves of the bovine vas deferens. Neuroscience 1987; 20:855-66.
100. Klarskov P. Enkephalin inhibits presynaptically the contractility of urinary tract smooth muscle. Br J Urol 1987;59:31-5.
101. Owman C, Stjernquist M. Origin, distribution and functional aspects of aminergic and peptidergic nerves in the male and female reproductive tracts. In: A Björklund, T Hökfelt, C Owman (eds.) Handbook of chemical neuroanatomy: the peripheral nervous system. Elsevier, Amsterdam, 1988; pp. 445-544.
102. Lacroix JS, Auberson S, Morel DR, Theodorsson E, Hökfelt T, Lundberg JM. Vascular control of the pig nasal mucosa: distribution and effect of somatostatin in relation to noradrenaline and neuropeptide Y. Regul Pept 1992;40:373-87.
103. Kaleczyc J, Scheuermann DW, Pidsudko Z, Majewski M, Lakomy M, Timmermans J-P. Distribution, immunohistochemical characteristics and nerve pathways of primary sensory neurons supplying the porcine vas deferens. Cell Tissue Res 2002;310:9-17.
104. Merighi A, Kar S, Gibson SJ, Ghidella S, Gobetto A, Peirone SM, et al. The immunocytochemical distribution of seven peptides in the spinal cord and dorsal root ganglia of horse and pig. Anat Embryol 1990;181:271-80.
105. Brown DR, Timmermans JP. Lessons from the porcine enteric nervous system. Neurogastroenterol Motil 2004;16:50-4.
106. Grundy D, Schemann M. Enteric nervous system. Curr Opin Gastroenterol 2005;21: 176-82.
107. Traub RJ, Hutchcroft K, Gebhart GF. The peptide content of colonic afferents decreases following colonic inflammation. Peptides 1999;20:267-73.
108. Anderson CR, Edwards SL, Furness JB, Bredt DS, Snyder SH. The distribution of nitric oxide synthase-containing autonomic preganglionic terminals in the rat. Brain Res 1993;614:78-85.
109. Andersson KE, Persson K. Nitric oxide synthase and the lower urinary tract: possible implications for physiology and pathophysiology. Scand J Urol Nephrol Suppl 1995; 175:43-53.
110. Anderson CR, Furness JB, Woodman HL, Edwards SL, Crack PJ, Smith AI. Characterisation of neurons with nitric oxide synthase immunoreactivity that project to prevertebral ganglia. J Auton Nerv Syst 1995;52:107-16.
111. Kuo DC, Hisamitsu T, De Groat, WC. A sympathetic projection from sacral paravertebral ganglia to the pelvic nerve and to postganglionic nerves on the surface of the urinary bladder and large intestine of the cat. J Comp Neurol 1984;226:76-86.